Linear Distributed Bragg Cavity Effects on Optical Limiting in Three-Level Media

JAMES H. ANDREWS[1], MADELINE SMOTZER[2], BRANDON LATRONICA[1], AND MICHAEL CRESCIMANNO[1,*]

[1] Youngstown State University, Dept. of Physics and Astronomy, Youngstown, OH, 44555
[2] The Ohio State University, Dept. of Chemistry, Columbus, OH, 43210
[*] Corresponding author: dcphtn@gmail.com

Compiled August 9, 2016

A lumped distributed Bragg reflector (DBR)-nonlinear layer-DBR system is used to explore how non-linear optical effects (in particular, optical limiting) are modulated by the dispersive character of the (optically linear) DBR. A three-level quantum optics model of the non-linear layer is used to find self-consistent numerical solutions to the (non-linear) optical transport in the composite system. We find that the intensity dependence of the real part of the index can be combined with the dispersion in the (linear) DBR to cause optical limiting even for materials that have only a saturated absorber (two-level) response. Further, we demonstrate that for a reverse saturable absorber, increases in narrow-band reflectivity of the composite system at higher intensities may reduce optical damage to the limiter.

OCIS codes: *(190.4360) Nonlinear Optical Devices; (270.4180) Multiphoton Processes; (050.5298) Photonic Crystals.*

http://dx.doi.org/10.1364/ao.XX.XXXXXX

1. INTRODUCTION

Optical limiters, *i.e.*, materials and composites that have reduced transmission with increasing optical power, are an interesting and useful application of wave transport and nonlinear optical (NLO) effects [1][2]. Historically, there have been three approaches to optical limiters, namely, intensity dependent absorption [3]-[5], reflection [6]-[8], or scattering [9]-[12]. In the case of the basic NLO process of saturable absorption (SA), usually the redistribution of populations associated with light absorption causes an increase in the transmission. By contrast, there is a rich history of intensity-dependent absorption limiters using bulk materials that display the opposite of saturation, *i.e.*, an increased rate of absorption with increasing intensity. They do so typically through multi-photon absorption in a process named reverse saturable absorption (RSA) [13]-[15]. In RSA materials, there is additional light absorption from excited states [13]-[17]. Although effective, these multi-photon absorptions tend to lead to highly-excited molecular states that are prone to molecular breakdown, thereby limiting the lifetime (and thus usefulness) of the limiter [18]. This problem also plagues limiters based on intensity-dependent scattering, leading to use of cascaded designs [19][20].

Limiters based on intensity-dependent reflection, on the other hand, are claimed to be significantly more immune to intensity-dependent breakdown [7][8]. In one idealization, [8][21], the limiter is a multi-layered film made of two materials, alternating either a linear optical element with a nonlinear refractive material, or alternating two materials with nonlinear refractive indices of opposite sign but, in either case, with matched indices of refraction at low intensities. High fluence illumination then causes a difference in the refraction index of the two layers, which results in an optical reflection band centered at a wavelength fixed during manufacturing by the layer thicknesses. In principle limiters of this type have the advantage of actually clamping the total transmitted light to a value determined by the NLO properties of the active layers (most limiters do not actually clamp the total transmitted intensity, but asymptote to a reduced, fixed transmission percentage). Practically, there are significant materials and manufacturing hurdles to making such an ideal, narrow-band limiter, and to our knowledge of the literature, there has been no laboratory demonstration of this methodology to date. Note also that this idealized system or any system based on multilayer interference effects only acts as a limiter over a fixed (potentially narrow) wavelength band.

A general lesson from the forgoing is that a potentially interesting route to make limiters arises by combining NLO response with the designed dispersion in a multi-layered photonic crystal. [22]-[29] To better understand the connection between limiting behavior, NLO response and one-dimensional photonic crystal structure, we focus on characterizing limiter behavior in a distributed Bragg reflector (DBR)-type photonic crystal. In particular we limit ourselves to a 'lumped' sys-

tem consisting of (nearly) matched linear dispersive multilayer (DBR) mirrors surrounding a central layer of a NLO material. We model this NLO layer as a three-level system with optical response (*i.e.*, homogeneous widths) much faster than the illumination pulse width so that, to first order, we can rely on the system's steady state response. This 'lumped' approach separates the NLO character (center layer only) from the DBR dispersion in order to illuminate the role played by each.

In Section 2 we review the basics of the NLO model for the center material and briefly describe our numerical method, which we then use in Section 3 to quantify the limiter behavior in a simple two-level (limit of the three-level quantum optics) model for the NLO material. Although the bulk optical nonlinearity of this two-level limit is only capable of saturable absorption, when it is combined with linear optical dispersion in the rest of the layered system, one finds narrow-band optical limiting. That section also contains a quantitative evaluation of the dependence of the limiting behavior on the detuning between the absorption band and the DBR reflection band and connects these results with the somewhat better studied phenomenology of folded DFB lasers.

Section 4 demonstrates the full three-level quantum optics model representing the optical response of the material in the center layer of the DBR sandwich. Such a three level quantum optics model has parameter ranges for which it explicitly exhibits RSA, and so could act as an *absorptive* limiter all by itself. When this material is used in the center of this DBR sandwich structure, the question arises: to what degree does the multilayer dispersion 'protect' the NLO material by selectively enhancing the reflection mode over the absorptive mode of the optical limiter made with this center layer? By using the model to quantify the reflection versus the absorption while acting as a limiter, and by quantifying the excited state populations in the center layer we address aspects of threshold and lifetime reduction in optical limiters consisting of RSA materials. We then conclude with a summary and discussion of future directions with experimental proposals for testing these findings.

2. MODEL AND METHODS:

Our model system for disentangling the contributions that both designed linear dispersion and non-linear optical response make to optical limiting is a DBR cavity, as shown in Fig. 1(a). The layered sections around the center material "C" form a linear optical binary photonic crystal composed of tens of nanometers thick alternating layers of different indices of refraction. Throughout we assume that these species are non-absorbing; the designed dispersion of the multilayer selectively enhances the optical limiting behavior of the entire composite system. The center layer "C" is composed of a monolithic (optically linear) material into which is embedded a nonlinear chromophore that absorbs and emits light. We model the NLO response of the chromophore through solving the steady state Maxwell Bloch equations (MBE) for a three level structure as show in Fig.1(b) (width parameters and decoherence rates are not shown for simplicity, but are included in the model).

Qualitatively, for just the bulk chromophore in "C," we can describe how the simple quantum optics model that we use supports limits in which the layer "C" displays either SA or RSA. In the limit that the state $|-1\rangle$ decouples from the transport (for example, if the coupling is small or the detuning D_1 is large) the two level system composed of the remaining states readily undergoes SA in the high intensity regime.

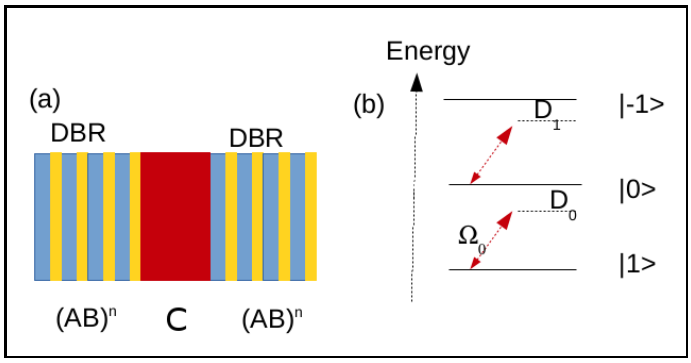

Fig. 1. (a) The DBR structure we study for limiting behavior. Note the mirrors are linear and the NLO response is in the center "C" layer only. (b) The level structure for the quantum optics model of the NLO material in layer "C."

Bulk (in the absence of the DBR) chromophore optical limiting behavior can be realized in a multilevel, multi-photon transition scheme (such as Fig. 1(b)) via RSA. Qualitatively, in the simple model here, RSA occurs by the cycling transition $|0\rangle \rightarrow |-1\rangle$ followed by $|-1\rangle \rightarrow |1\rangle$ via quick decay (note mixed parity states in the model). This process reduces the population buildup in $|0\rangle$ thereby reducing the stimulated emission that leads to SA. Further, for a range of parameters, the cycling works so well that transmission is actually lower at high intensities than at low intensities, *i.e.* the optical limiting behavior. In many dyes, while the molecule is in the $|-1\rangle$ state there are likely to be many states to which it can decay that lead to disintegration pathways or non-reversible structural changes that greatly affect its optical properties. Our model allows us to compute the population in the $|-1\rangle$ state as a function of light input intensity and wavelength (see for example, Fig. 3(d)) which we use to compare the dye disintegration rates for limiters with and without using DBR layers. We can also compute the population in the $|0\rangle$ state, as in Fig. 2(c) but, because it is lower energy, we do not relate that population to dye functional lifetime. We show below how the DBR structure with an RSA material as "C" can shift this absorption-based RSA optical limiting to one in which reflection is enhanced at high intensities, and we quantify the associated reduction in the population in state $|-1\rangle$, suggesting an effective lengthening of the limiter's functional lifetime.

Quantitatively, we model optical transport through the DBR by transfer matrices (for a review of the technology and its application, see [29] [30]). In 1-d transport along the $\hat{z}$ axis, in the field basis $\vec{v} = (E_x, B_y)$ for fields in which $(1, n)$ is a right-traveling wave and $(1, -n)$ is a left-traveling wave, the fields $\vec{v}_i$ at the left side of a monolithic dielectric element of (complex) index of refraction n and thickness x are related to the fields at the right side of the monolith as $\vec{v}_{i+1} = M_i \vec{v}_i$ where the transfer matrix M_i is

$$M_i = \begin{bmatrix} \cos nkx & \frac{1}{n}\sin nkx \\ n \sin nkx & \cos nkx \end{bmatrix} \quad \textbf{(1)}$$

Note that $det(M_i) = 1$ and thus that M_i^{-1} is just M_i with $x \rightarrow -x$, as expected (we focus on a single polarization state throughout). The utility of using the transfer matrices is that the transport of light through a composite is equal to a single transfer matrix that is just the sequential product of the transfer

matrices of each of the layers, $M_{tot} = \Pi_i M_I = \begin{bmatrix} a & b \\ c & d \end{bmatrix}$, and that in the chosen basis, for the composite in air, the overall transmission and reflection amplitudes are, respectively,

$$t = \frac{2}{a+d-b-c} \qquad r = \frac{b-c}{a+d-b-c}. \tag{2}$$

For layer "C," the NLO element's transfer matrix, we compute the layer's mean index of refraction by first taking a single, mean value I for the intensity in that layer given an intensity I_0 incident from the air upon the whole composite structure. In that I, we solve the quantum optics model for the idealized chromophore whose level structure is that of Fig. 1(b) using,

$$\partial_t \rho = 0 = -i[H,\rho] + \mathcal{L}\rho \tag{3}$$

for the density matrix ρ of the system, via, a steady state solution. We work in the rotating wave approximation (RWA). In that frame the Hamiltonian H includes diagonal detunings and off-diagonal Rabi frequencies proportional to the product of the dipole matrix elements for that off diagonal element and the square root of I. The $\mathcal{L}\rho$ term contains all the relaxation parameters such as population and coherence decay rates.

After solving Eq. (3) for steady state $\partial_t \rho = 0$ (an approximation warranted by comparing the widths and decay rates for the model Fig. 1(b) with the assumed optical pulse widths), we assemble the mean (complex) index of refraction for the layer "C" using

$$n_c^2 = n_{c0}^2 + N\xi(c_{01}\rho_{01} + c_{-10}\rho_{-10})/\Omega, \tag{4}$$

where n_{c0} is the 'background' index of refraction (throughout we take that index to be constant and equal to one of the indices of the DBR layers) of the monolithic material into which the chromophores at volumetric density N have been uniformly dispersed. The ξ is, up to factors of ϵ_0 and $\hbar$, an average dipole matrix element and the c_{01} and c_{-10} are the (constant) coupling factors (generalized Clebsch-Gordon coefficients) for the respective transitions driven by the light where $I \sim \Omega^2$.

The simple three-level model captures other phenomena expected of real media. For example, if D_0 and D_1 are sufficiently close to one another (their difference is less than the ρ_{01} decoherence rate), the RSA behavior disappears into global SA behavior. Conversely, if these detunings in the dye are wildly different, the quantum optics model reduces effectively to a two-level system, and again RSA $\rightarrow$ SA. Finally, if parameters are chosen so that the system displays RSA but the intensity is increased further, eventually RSA $\rightarrow$ SA again, as expected on physical grounds.

Thus, the non-linear index of the medium through the intensity dependence of the coherences ρ_{01} and ρ_{-10} actually changes the transmission of the whole system, and, in particular, changes the assumed intensity in region "C." For each wavelength and input intensity I_0, we numerically find a self-consistent approximate solution to this NLO transport problem by iteration. That is, starting from the naive guess $I = I_0$ we use Eq. (4) to, via Eq. (2), find the transmitted light amplitude. We then invert the transfer matrix associated with the final DBR stack and use it to get an estimate for the field at the output facet of region "C." We then assume linear transport in that region to arrive at a new average intensity $I \neq I_0$ in that "C" region. We then use this new average intensity to update the index for region "C" and solve again the transport problem, then find the new output intensity to again update the internal field in "C" and keep doing so until this iterative process converges, at which point we have arrived at an approximate self-consistent solution of the non-linear transport.

This numerical approach does not avoid the optical multi-stability that is generic to loaded cavities (which this system approximates). Consequently, we find that for some parameter choices this method does not converge, but instead toggles across a set of values. Were such structures to eventually find their way into practical passive optical limiters, this generic multi-stability, as well as angular acceptance and other issues, could present design challenges. Here we focus on demonstrating the connection between dispersion and optical limiting with the goal of building up intuition regarding these compromises. Happily, it is quite easy to find a broad range of realistic parameters for this system that do not result in multi-stability. Restricting our investigations to this range is sufficient for the purposes of this study.

Finally, we alert the reader to the fact that because our goal is an elucidation of the underlying physical effects and not optimization, we have throughout made rather generic choices for system parameters and, as a result of this approach, the expected optical limiting performance improvement from the inclusion of the DBR sections is modest. Because of the ease of manufacturing, low cost and post-processibility of co-extruded polymeric DBR films,[33][34] all the simulations described here assume the optical constants for poly-methylmethacrylate (PMMA)/polystyrene(PS) multilayer stacks for the DBR and PMMA for the monolith (of index n_{c0} of Eq.(4)) "C" layer into which the chromophores are uniformly distributed.

3. OPTICAL LIMITING IN A SATURABLE ABSORBER

In bulk for a two-level system, as the intensity climbs, so does the population in the excited state, and the material enters optical saturation. We reduce the ratio of generalized Clebsch-Gordon coefficient's c_{-10}/c_{01} in our model to render it effectively a two-level model. For that choice, in the high intensity limit, the material's dipolar response decreases as stimulated emission starts to dominate due to saturation. This SA behavior means that the material becomes more transparent with increasing input intensity, which is exactly the opposite of optical limiting. We now show, perhaps somewhat surprisingly, that such a material used in the lumped composite system described above can act as a narrow-band optical limiter by becoming more reflective and thus less transparent at higher intensities. Below, we explain this in terms of the intensity-dependent changes in the real part of the index, and the associated increased reflectivity at certain wavelengths as the intensity increases, similar in spirit to the idealization in [8][21], but arguably more practicable.

We plot in Fig. 2(a) the ratio of the transmission at low intensity to the transmission at high intensity (solid red trace) as a function of wavelength for a DBR sandwich in which the central layer has generic parameters that lead to SA, but at an absorption band detuned from the reflection band of the DBR (the low intensity transmission of the system is shown as a dashed (green) line). The thicknesses of the individual DBR layers (48 in each DBR) are each 70 nm, whereas layer "C" is 300 nm thick. As one can see, the ratio decreases from unity as one moves into the absorption band of the "C" layer, as SA ensues. In this metric, wavelengths where the aforementioned ratio is greater

than unity correspond to limiter-type behavior. At 434 nm, in the transmission trace for the composite, inside the DBR reflection band there is a transparency resonance, sometimes referred to in the literature as a interband defect [35]-[37]. Interband defects, which may be thought of as generalized Fabry-Perot cavity modes in this optical geometry, are associated with pronounced reductions in the group velocity and large dispersive effects. Consistent with that, Finite-Difference, Time-Domain (FDTD) simulations also indicate that the spatial map of the intensity in these modes can be significantly enhanced in the "C" layers, and, in this application, can lower the optical limiting threshold of the composite as compared to that of the bulk material.

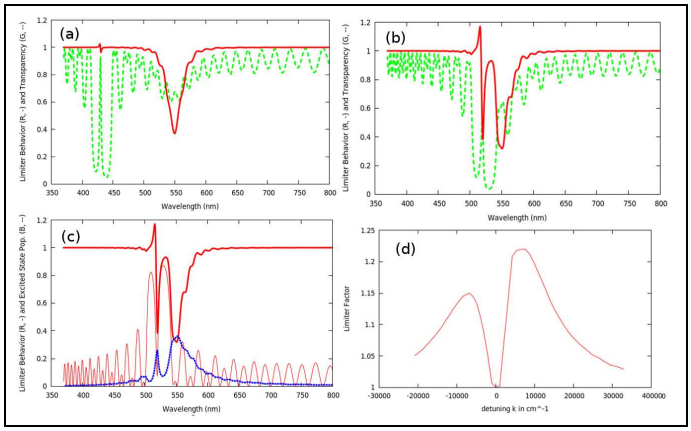

Fig. 2. (a) Ratio of transmission at low intensity to that at high intensity for a DBR reflection band detuned from the NLO material in "C"'s first optical transition $|1\rangle \rightarrow |0\rangle$ (solid red trace). The net transmission is shown as a dashed green trace. (b) Same system, illumination and traces as in (a), but with the layer thicknesses changed so that the DBR reflection band now partially overlaps with the $|1\rangle \rightarrow |0\rangle$ transition. Limiting behavior (Ratio > 1) occurs across a range of frequencies, across the reflection band up to the defect location. (c) The reflection (red, thin) and the population in the excited state $|0\rangle$ (blue, thick dash) for the same parameters as in (b). (d) The maximum of the limiting effect (transmission ratio at low intensity to that at high intensity) as a function of the detuning between "C" layers $|1\rangle \rightarrow |0\rangle$ transition and the DBR reflection band center. To make this last graph, we have held the DBR layers and the center layer "C" thickness fixed and slewed just the frequency of the $|1\rangle \rightarrow |0\rangle$ transition.

To highlight the effects of dispersion in this structure for modulating the SA into limiting behavior, Fig. 2(b) shows the same system under the same illumination with the only change being the layer thicknesses in the system has been changed so that its reflection band and the absorption band partially overlap. In SA, not only does the absorption index change with intensity, but the real part of the index does as well, changing the reflection band location and leading to decreased transmission with intensity across part of the reflection band. Figure 2(c), for the same system, plots the reflection and absorption percentages. For comparison, for the system in Figure 2(a), the reflection is below 20% across the absorption resonance. Again, here we have made no effort to optimize the limiting behavior the structure, as we are here just concerned with demonstrating the generic effects.

The forgoing indicates the profound effect that the optical non-linearity of the central region can have on the optical transport of the composite. With a nod towards design, in Figure 2(d) we plot, for a fixed high input intensity, the maximum limiting factor (typically very near the wavelength of the interband defect mode) as a function of the detuning between the absorption feature in the dye (the $|1\rangle \rightarrow |0\rangle$ resonance) and the DBR reflection band center. We do so by holding all the structure (species and physical thicknesses) fixed and just slewing the $|1\rangle \rightarrow |0\rangle$ transition of the material in the "C" layer. The fact that the limiting effect is largest when slightly detuned (to either side) of the resonance indicates that it is the change wrought by the intensity dependence of the real part of the index that drives this limiter enhancement.

Intensity-dependent index change also explains the shape of the reflectivity ratio. For the chromophore transmission centered about 550 nm as in Figure 2, we expect the index of refraction to exhibit anomalous dispersion across the transition such that it has a higher index at longer wavelengths (just below the transition) and lower index at wavelengths shorter than 550 nm (again, close to the transition), but normal dispersion away from the transition. As the intensity increases and the chromophores start to saturate, the real part of the index in the center layer increases at wavelengths smaller than 550 nm, while it decreases at longer wavelengths. This means that the band and band defect move to higher (vacuum) wavelengths when the band is red detuned from the chromophore's absorption peak, and, conversely, move to shorter (vacuum) wavelengths when the reflection band is blue detuned from the absorption transition. Given the shape of the reflection band's transmission (Fig. 2(a), 400-450 nm), one can see that shifting it to the right leads to the reflectivity ratio's dispersive feature as shown in Fig.2(a) and 2(b). Though not shown, our simulations show that for a reflection band at longer wavelengths than the chromophore's transition, the shape of the dispersive feature flips, consonant with the above described changes in the real part of the index in SA with increased intensity.

DBR mirrors are often employed in laser designs, and from that literature [38][39] there is an expectation for the laser threshold to depend on the group velocity delay from the various choices of layer orderings. For a thin central "C" layer, the different ordering choices lead to different field intensities in the center layer. In the laser case, the higher fields at "C" are associated with smaller group velocity across the structure and correspondingly lower folded DBR laser thresholds. Our model indicates that the highest absorption in the layer "C" occurs when we 'fold' the structure in Figure 1(a) along the low index component (that is, with $n_A < n_B$ and in the structures $(BA)^n C(AB)^n$ where n indicates the number of layer pairs on each side of the center layer).

Importantly, we find that regardless of the two fold choices (whether the structure is folded on the high index material OR the low index material), the peak reflectivity ratio (the figure of merit for optical limiting that we have graphed as a function of wavelength in Figs. 2(a,b)), is virtually unchanged with respect to this fold choice. This indicates not only that the limiting effect on the in-band defect is due to change in the real part of the index of the non-linear element "C", but that for dyes in which absorption leads to damage or destruction, there are relevant optical design options for these DFB-sandwich limiters. We note further that our simulations indicate these conclusions are qualitatively unaffected by the detuning between the band and the absorption center wavelength; that is, for a fixed detun-

ing (red or blue) with respect to the absorption line, the optical geometry in which the fold is on the high index material minimizes the absorption in the "C" layer for the same reflectivity ratio (limiter figure of merit).

Ref. [39] includes a study of relative refractive index orderings in folded Distributed Feedback (DBF) Lasers. The fold creates a in-band defect state associated with large dispersive effects. In folded DFB lasers, the gain medium is in every other layer, and there are four distinct design choices for the folded structure, namely whether the fold is the low index material or the high index one and which material (high index or low) has the gain. For those structures, as in the ones we study for optical limiting, the largest gain (in the case of lasers) or absorption (in the case of limiters) occurs when the structure is folded on the low index material. Although our system only has loss in the center region "C" (unlike the folded DFB), the spatial structure of the defect mode for the DFB reveals that the field intensity is largest in the fold region, so the folded DFB and folded DBR have the same phenomenology with respect to the choice of how the index of refraction of the center (fold) layer compares to the surrounding layers and in what material the gain/loss resides.

4. LIFETIME EXTENSION FOR RSA OPTICAL LIMITERS

By increasing the ratio c_{-10}/c_{01} in the forgoing quantum optics model, one can change its high intensity response from SA into RSA. This is shown in Fig.3(a), which is the analog of Fig. 2(a) with that increase and for which the $|0\rangle \rightarrow |-1\rangle$ splitting is at 533 nm (note the broad bulk RSA response extending from 470 nm to 530 nm.) As the DBR is tuned onto the resonance(s) in the non-linear element "C," the limiting effect is correspondingly modulated (Fig. 3(b)). This modulation is associated with changes in the reflectivity as a share of the total light impinging on the composite system, as indicated further in Fig. 3(c) whose dashed (green) line is the reflectivity ratio (equal to the reflectivity at high intensity divided by reflectivity at low intensity). There are indications in prior literature that combining a DFB or DBR structure with an optical limiting chromophore can modulate the reflectivity in such a way that the intensity of light in the non-linear layers stays low enough to substantially extend the lifetime of the active chromophore. As already noted, typically multi-photon absorption allows chromophore molecule to have enough energy to access many additional states, including dissociative ones and ones that render the molecule permanently optically inactive. We did not consider this problem in the SA case because typical chromophores are comparatively more stable at the first excited state. We test this further in our simulations for the RSA system by determining the mean second excited state population as a function of the wavelength and light input, with and without the DBR layers. In this way we can rather directly assay the potential of for preserving the lifetime of the active layer by combining linear dispersion with NLO limiting.

In Fig. 3(d), the long dashed trace (70 nm thick DBR layers as in (a), reflection band at 420 nm-450 nm) indicates that far off the $|1\rangle \rightarrow |0\rangle$ resonance one can still build up population in the $|-1\rangle$ (second excited state) because at the in-band defect mode the intensity at the center layer is enhanced. Thus note that the defect mode assisted limiting behavior in Fig.3(a) is absorption dominated (compare with the RSA peaks). Conversely, the short dashed trace in Fig. 3(d) (82 nm thick DBR layers as

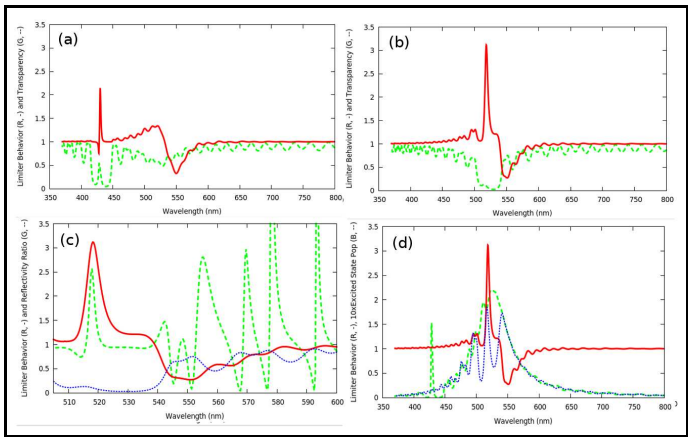

Fig. 3. (a) For material with RSA, the plot of the ratio of transmission at low intensity to that at high intensity (solid red trace) for a DBR reflection band detuned from the NLO material lowest energy optical transition. Shown as a dashed green trace is the net transmission at low intensity. Note that the material, displaying RSA, actually darkens with intensity around 520-540 nm (b) Same system, illumination and traces, but with the layer thicknesses of the DBR changed so that the DBR reflection band now partially overlaps with the $|1\rangle \rightarrow |0\rangle$ transition. (c) The individual reflection and absorption percentages for the system that leads to the transmission ratio of (b). (d) A comparison of the second excited level population ($|-1\rangle$) as a function of the wavelength for the system shown in Fig. 3(b) (blue, fine dash) and Fig. 3(a) (green, broad dashed line).

in (b), reflection band from 470 nm-520 nm), the second excited state's ($|-1\rangle$) population is the same as in the long dashed case (*i.e.* the RSA peak of the bulk material), but the limiter effect is greater. The difference between these cases is the intensity dependent increase in the reflectivity there, as corroborated in Fig. 3(c) where the dark dashed line is the ratio of the reflectivity of the system at high intensity over that same reflectivity at low intensity.

This suggests the potential usefulness of carefully combining linear dispersion with optical limiters. For optical limiting, one is not limited to using only the imaginary part (absorption) of the index; the non-linear changes in the real part (refraction) of the index can also be harnessed to achieve greater optical limiting, and there are important advantages to doing so. The above constitutes a demonstration of this straightforward idea in the rigorous context of a fundamental quantum optics model for the non-linear response of the chromophores.

5. CONCLUSION

One of the main themes that we have stressed throughout this paper is how combining linear dispersion in one part of the optical structure with non-linear optical effects in the rest of the structure can lead to a rich phenomenology that includes optical limiting, even in a materials that would otherwise only exhibit SA in the bulk, *i.e.*, whose default behavior is the opposite of optical limiting. We have shown that some of the observed optical limiting behavior can be related to group velocity changes associated with the optical superstructure the non-linear elements find themselves in, and that the associated modulations of the optical limiting behavior is qualitatively the same as the better known structural dependence of lasing effi-

ciency in DBR lasers. [38][39]

We are currently investigating these theoretical expectations in experiments using co-extruded polymeric Bragg reflectors, of significant recent interest [33][34] for their quality, flexibility, modularity, post-processing capability, low cost and broad material compatibility. Baseline experiments are underway studying the optical limiting behavior in PS-PMMA based DBR's around a "C" region that is a dye-laden PMMA spun-coated onto the same polymer DBR, structurally identical to the optical geometries described theoretically in this paper.

National Science Foundation (NSF), Science and Technology Center for Layered Polymeric Systems (DMR 0423914). The authors thank N. Dawson and K. Singer for technical comments.

REFERENCES

1. L. Tutt and T. Boggess, "A review of optical limiting mechanisms and devices using organics, fullerenes, semiconductors and other materials," Prog. Quantum Electron. **17**, 299-338 (1993).
2. R. C. Hollins, "Materials for optical limiters," Solid State Mater. Sci. **4**, 189-196 (1999).
3. Y. Huang, G. Siganakis, M. G. Moharam, and S.-T. Wu "Broadband optical limiter based on nonlinear photoinduced anisotropy in bacteriorhodopsin film," Appl. Phys. Lett. **85**, 5445-5447 (2004).
4. T. H.Wei, D. J. Hagen, M. J. Sence, E. W. Van Stryland, J. W. Perry, and D. R. Coulter, "Direct measurements of nonlinear absorption and refraction in solutions of phthalocyanines," Appl. Phys. B. 54, 46-51 (1992).
5. J. S. Shirk, R. G. S. Pong, F. J. Bartoli, and A. W. Snow, "Optical limiter using a lead phthalocyanine," Appl. Phys. Lett. **63**, 1880-1882 (1993).
6. M. Scalora, J. P. Dowling, C. M. Bowden, and M. J. Bloemer, "Optical limiting and switching of ultrashort pulses in nonlinear photonic band gap materials," Phys. Rev. Lett. **73**, 1368-1371 (1994).
7. P. Tran, "Optical limiting and switching of short pulses by use of a nonlinear photonic bandgap structure with a defect," J. Opt. Soc. Am. B **14**, 2589-2595 (1997).
8. L. Brzozowski and E. H. Sargent "Nonlinear distributed-feedback structures as passive optical limiters," J. Opt. Soc. Am. B **17**, 1360-1365 (2000).
9. G.-K. Lim, Z.-L. Chen, J. Clark, R. G. S. Goh, W.-H. Ng, H.-W. Tan, R. H. Friend, P. K. H. Ho, and L.-L. Chua, "Giant broadband nonlinear optical absorption response in dispersed graphene single sheets," Nature Photonics **5** 554-560 (2011).
10. Y.-P. Sun, J. .E. Riggs, K. B. Henbest, and R. B. Martin, "Nanomaterials as optical limiters," J. Nonlinear Opt. Phys. & Mater. **9**, 481-503 (2000).
11. Guisheng Pan, R. Kesavamoorthy, and Sanford A. Asher, "Optically nonlinear Bragg diffracting nanosecond optical switches," Phys. Rev. Lett. **78**, 3860-3863 (1997).
12. S. Husaini, J. E. Slagle, J. M. Murray, S. Guha, L. P. Gonzalez, and R. G. Bedford, "Broadband saturable absorption and optical limiting in graphene-polymer composites," Appl. Phys. Lett. **102**, 191112 (2013).
13. C. W. Spangler, "Recent development in the design of organic materials for optical power limiting," J. Mater. Chem. **9**, 2013-2020 (1999).
14. M. Calvete, G. Y. Yang, and M. Hanack, "Porphyrins and phthalocyanines as materials for optical limiting," Synthetic Metals **141** 231-243 (2004).
15. S. Sreeja, S. Sreedhanya, N. Smijesh, R. Philip and C. I. Muneera, "Organic dye impregnated poly(vinyl alcohol) nanocomposite as an efficient optical limiter: structure, morphology and photophysical properties," J. Mater. Chem. C, **1**, 3851-3861 (2013).
16. J. S. Shirk, R. G. S Pong, S. R Flom, F. J. Bartoli, M. E. Boylez and A. W. Snow, "Lead phthalocyanine reverse saturable absorption optical limiters," Pure Appl. Opt. **5**, 701-707 (1996).
17. C. Gayathri, A. Ramalingam, "Studies of third-order optical nonlinearities and optical limiting properties of azo dyes," Spectrochimica Acta Part A **69**, 980-984 (2008).
18. H. Zhang, D. E. Zelmon, L. Deng, H.-K. Liu, and B. K. Teo, "Optical limiting behavior of nanosized polyicosahedral gold-silver clusters based on third-order nonlinear optical effects," J. Am. Chem. Soc. **123**, 11300-11301 (2001).
19. Y. Chen, M. Hanack, Y. Araki and O. Ito, "Axially modified gallium phthalocyanines and naphthalocyanines for optical limiting," Chem. Soc. Rev. **34**, 517-529 (2005).
20. Y. Xiong, L. Yan, J. Si, W. Yi, W. Ding, W. Tan, X. Liu, F. Chen, and X. Hou "Cascaded optical limiter with low activating and high damage thresholds using single layer graphene and single-walled carbon nanotubes," J. Appl. Phys. **115**, 083111 (2014).
21. B. Y. Soon, J. W. Haus, M. Scalora, and C. Sibilia, "One-dimensional photonic crystal optical limiter," Opt. Express **11**, 2007-2018 (2003).
22. M. C. Larciprete, C. Sibilia, S. Paoloni, M. Bertolotti, F. Sarto, and M. Scalora, "Accessing the optical limiting properties of metallo-dielectric photonic band gap structures," J. Appl. Phys. **93**, 5013-5017 (2003).
23. J. H. Vella, J. H. Goldsmith, A. T. Browning, N. I. Limberopoulos, I. Vitebskiy, E. Makri, and T. Kottos, "Experimental realization of a reflective optical limiter," Phys. Rev. Appl. **5**, 064010 (2016).
24. E. Makri, T. Kottos, and I. Vitebskiy "Reflective optical limiter based on resonant transmission," Phys. Rev. A **91**, 043838 (2015).
25. D. Pelinovsky, J. Sears, L. Brzozowski, and E. H. Sargent, "Stable all-optical limiting in nonlinear periodic structures. I. Analysis," J. Opt. Soc. Am. B **19**, 43-53 (2002).
26. R. Wang, J. Dong, and D. Y. Xing "Dispersive optical bistability in one-dimensional doped photonic band gap structures," Phys. Rev. E **55**, 6301-6304 (1997).
27. M. Centini, C. Sibilia, M. Scalora, G. D. Aguanno, M. Bertolotti, M. J. Bloemer, C. M. Bowden, and I. Nefedov, "Dispersive properties of finite, one-dimensional photonic band gap structures: Applications to nonlinear quadratic interactions," Phys. Rev. E **60** 4891-4898 (1999).
28. J. Zhang, N. Coombs, and E. Kumacheva, "A new approach to hybrid nanocomposite materials with periodic structures," J. Am. Chem. Soc. **124**, 14512-14513 (2002).
29. F. J. Lawrence, C. M. de Sterke, L. C. Botten, R. C. McPhedran, and K. B. Dossou, "Modeling photonic crystal interfaces and stacks: impedance-based approaches," Adv. Opt. Photon. **5**, 385-455 (2013).
30. P. Yeh, *Optical Waves in Layered Media; Wiley Series in Pure and Applied Optics* (Wiley,1998).
31. Y. Zhang, S. Qiao, L. Sun, Q. W. Shi, W. Huang, vanadium dioxide film deposited by sol-gel method," Opt. Express **22**, 11070-11078 (2014).
32. P. Yeh, "Optics of anisotropic layered media: A new 4 x 4 matrix algebra," Surf. Sci. **96**, 41-53 (1980).
33. T. Kazmierczak, H. Song, A. Hiltner, E. Baer, "Polymeric one-dimensional photonic crystals by continuous coextrusion," Macromol. Rapid Commun. **28** 2210-2216 (2007).
34. M. Ponting, T. M. Burt, L. T. J. Korley, J.H. Andrews, A. Hiltner, and E. Baer, "Gradient multilayer films by forced assembly coextrusion," Indust. & Eng. Chem. Res., **49**, 12111-12118 (2010).
35. J. P. Dowling, M. Scalora, M. J. Bloemer and C. M. Bowden, J. Appl. Phys., "The photonic band-edge optical diode," **75**, 1896–1899 (1994).
36. D. R. Smith, R. Dalichaouch, N. Kroll, S. Schultz, S. L. McCall and P. M. Platzman, "Photonic band structure and defects in one and two dimensions," J. Opt. Soc. Am. B **10**, 314–321 (1993).
37. H. Song, K.D. Singer, J. Lott, J. Zhou, J.H. Andrews, E. Baer, A. Hiltner, and C. Weder, "Continuous Melt Processing of All-Polymer Distributed Feedback Lasers," J. Mater. Chem. **19**, 7520–7524 (2009).
38. K. D. Singer, T. Kazmierczak, J. Lott, H. Song, Y. Wu, J. H. Andrews, E. Baer, A. Hiltner, and C. Weder, "Melt-processed all-polymer distributed Bragg reflector laser," Opt. Express **16**, 10358-10363 (2008).
39. J. H. Andrews, M. Crescimanno, K. D. Singer, E. Baer, "Melt-processed polymer multilayer distributed feedback lasers: progress and prospects," J. Poly. Sci. B: Poly. Phys **52**, 251-271 (2014).